Geometric morphology of cellular solids

Bernd R. Schlei*[a], Lakshman Prasad[b], Alexei N. Skourikhine[b]

[a]Los Alamos National Laboratory, Theoretical Division, T-1, MS B221,
Los Alamos, NM 87545, U.S.A.
[b]Los Alamos National Laboratory, Nonproliferation and International Security, NIS-7, MS B221,
Los Alamos, NM 87545, U.S.A.

ABSTRACT

We demonstrate how to derive morphological information from micrographs, i.e., grey-level images, of polymeric foams. The segmentation of the images is performed by applying a pulse-coupled neural network. This processing generates blobs of the foams walls/struts and voids, respectively. The contours of the blobs and their corresponding points form the input to a constrained Delaunay tessellation, which provides an unstructured grid of the material under consideration. The subsequently applied Chordal Axis Transform captures the intrinsic shape characteristics, and facilitates the identification and localization of key morphological features. While stochastic features of the polymeric foams struts/walls such as areas, aspect ratios, etc., already can be computed at this stage, the foams voids require further geometric processing. The voids are separated into single foam cells. This shape manipulation leads to a refinement of the initial blob contours, which then requires the repeated application of the constrained Delaunay tessellation and Chordal Axis Transform, respectively. Using minimum enclosing rectangles for each foam cell, finally the stochastic features of the foam voids are computed.

1. INTRODUCTION

Hydrodynamic models are used to model the response of cellular materials (e.g., polymeric foams) to highly dynamic, cyclic, and non-equilibrium-inducing loading conditions involving large strains and large strain rates. For the description of cell-level stresses such models may involve a deterministic single-cell mechanical model and employ probability functions[1], which are used to describe the stochastic nature of the foam structure and polymeric material properties. Details such as cell dimensions, shapes, orientations, strut/wall thickness, etc., may be used as independent variables upon which probability functions depend.

Polymeric foams are viewed as consisting of two separate but interacting materials – the cellular polymer and the permeating fluid (e.g., usually air) – each with its own distinct physical properties. Therefore, it is sufficient to decompose a given grey-level image of a cross-section of such a material into regions of the cellular polymer ("struts and/or walls") and the permeating air ("voids"), respectively.

This paper is structured as follows: In the next section we explain first the binary image decomposition by using a pulse-coupled neural network[2] (PCNN). Then we explain in more detail the contour extraction of the image blobs. We demonstrate the transform of the spectral pixel information of a micrograph into an affine geometric description by applying a constrained Delaunay tessellation[3] (CDT) and a subsequent Chordal Axis Transform[4,5] (CAT). The latter transform allows us to distinguish between structurally (morphologically) important and unimportant shape features of the polymeric foams struts/walls and voids, respectively. The statistical shape properties of the foams struts and walls can be computed at this stage already very reliably. On the contrary, the foams void consists of a complicated network of merged, mostly convex shaped, single void cells. Since we would like to capture the statistical nature of these individual void cells, rather than the shape features of the foams permeating fluid as a whole, we are faced with the task of a proper shape break-up of the foams large void. We are going to explain, how we accomplish this shape decomposition, which then leads to a refinement of the initial image blob contours. We repeat the application of the CDT and the CAT, respectively. For the final computation of the voids single cells statistical properties we are using minimum enclosing rectangles for extracting aspect ratios, in addition to the morphological information already provided by the CAT. This latter step will conclude our morphological analysis of cellular solids.

* E-mail: schlei@lanl.gov; phone 1 505 667-6740; fax 1 505 665-5757; http://www.nis.lanl.gov/~bschlei/; Los Alamos National Laboratory, Theoretical Division, T-1, P.O. Box 1663, MS B221, Los Alamos, NM 87545, U.S.A.

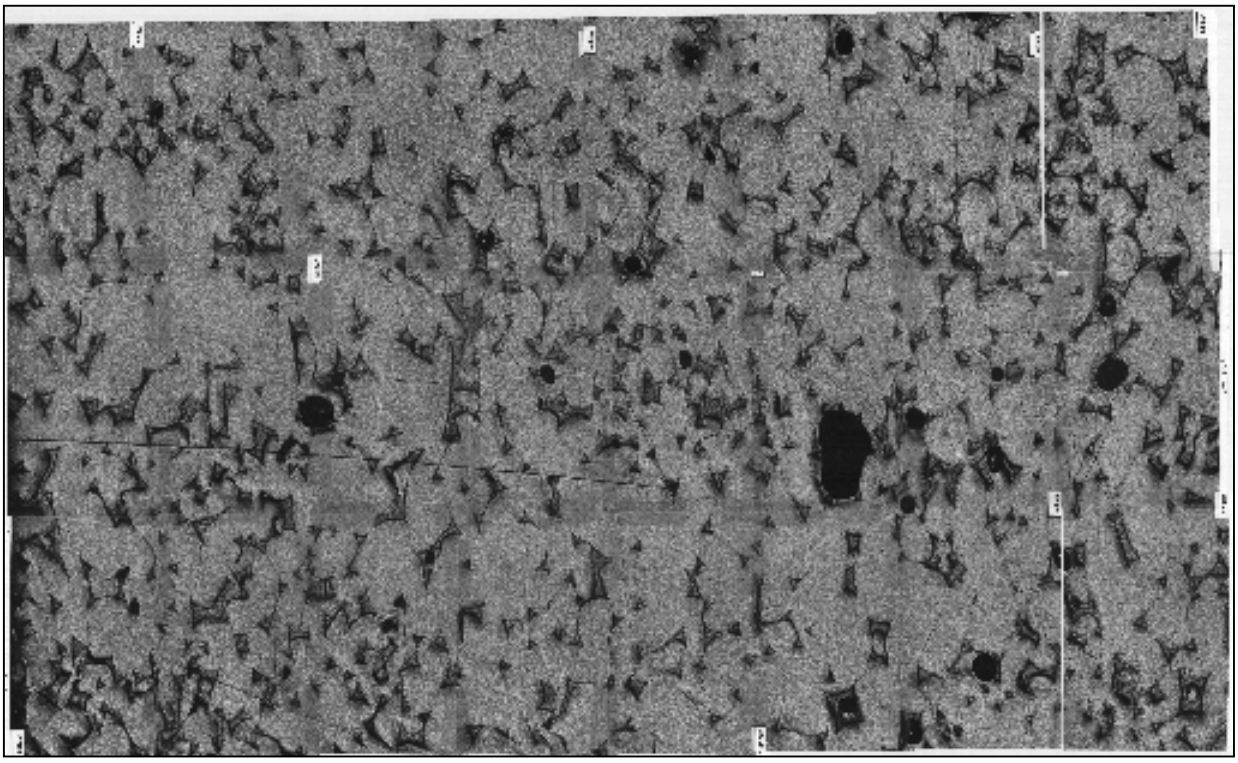

Figure1: Original Image

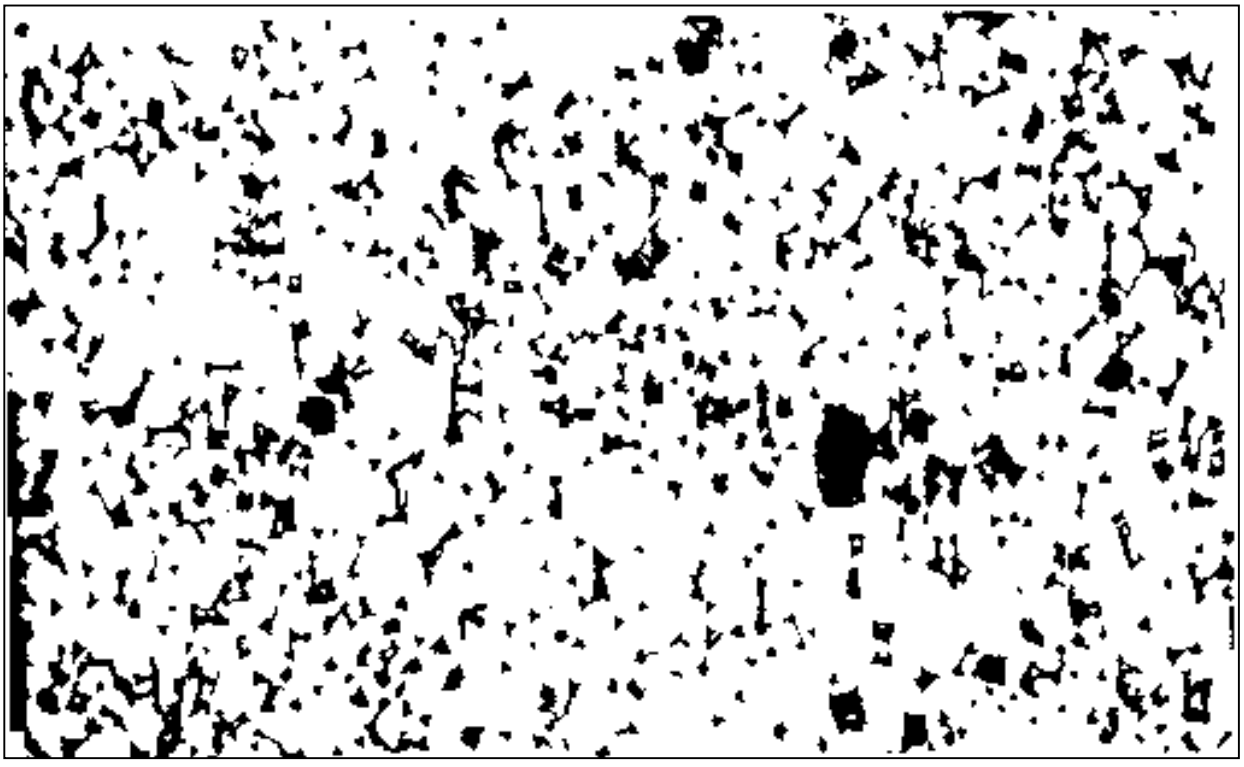

Figure 2: Segmented image

2. IMAGE PROCESSING

In this section we are processing a micrograph of a polymeric foam with pixel based and geometry based techniques, respectively. The following subsections address the tasks of image segmentation, contour extraction, region tessellation, extraction and classification of morphological shape features, contour refinement, and the extraction of statistical shape properties.

2.1 Image segmentation

The pulse-coupled neural network model of the cat visual cortex[6,7] has been proven to have very interesting properties for the purpose of image processing. In Ref. 2, the micrograph[8] as shown in Fig. 1 was processed using a PCNN. In this previous work, we were able to demonstrate that the PCNN is a useful tool for image preprocessing such as image denoising and segmentation. The integration of smoothing, segmentation, and the addition of output binary images enabled us to automate the process of processing images of cellular solids such as the polymeric foam considered here. Manual intervention was only necessary in order to select which image among those generated was the best. We hope to automate this selection process in the future as well. The image segmentation by itself was performed automatically. The result of our PCNN application for the micrograph in Fig. 1 is shown in Fig. 2 (cf., Ref. 2 for further detail).

In the following, we show for the sake of illustration a cropped sub-image of Fig. 2 with increased magnification (cf., Fig. 3). However, all statistical evaluations given below in this paper are made while using the whole segmented image as shown in Fig. 2.

2.2 Contour extraction

The next step after the image segmentation is the contour extraction of the generated blobs. For the material science application under consideration we initially desire blob contours, which are non-degenerate, i.e., which always enclose an area larger than zero, and which never cross or overlap each other. Furthermore, the contours should be oriented with respect to the objects and their possible holes.

In Fig. 4, we show dilated contours as generated by the algorithm[9], which is described in the paper by Schlei et al.[10] and which fulfills all of the above stated requirements for the contours. Our code uses a bi-level image (cf., black and white image Fig. 4) as input and generates closed and dilated image blobs as output (cf. Fig. 5). This is done in two steps. First, the neighborhood of each white image pixel is evaluated for its contribution to an edge list. In the second step, the edge elements are linearly connected to closed contours, and finally the edge coordinates are dilated. In our example shown in Fig. 4, we

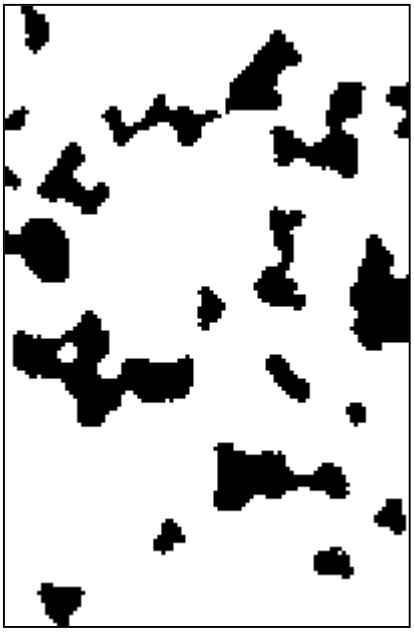

Figure 3: Enlarged region of blobs

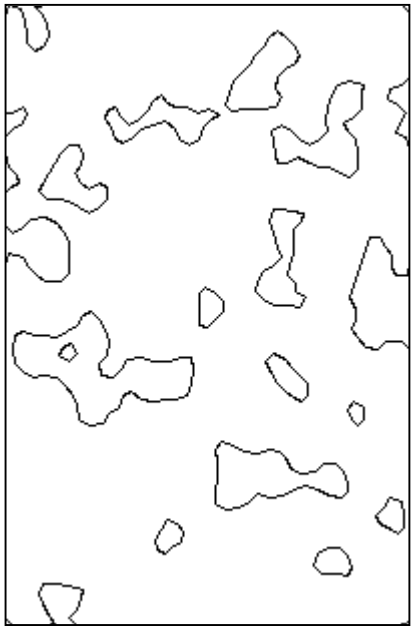

Figure 4: Contour enclosure

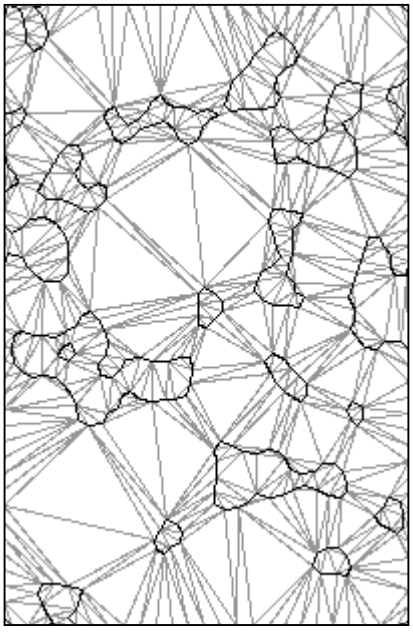

Figure 5: Delaunay tesselation

have also reduced the number of contributing edge points, so that the subsequently generated tessellation network is not too dense for our illustration purposes. However, the full calculations take into account all edge points. We have reduced the number of edge points by replacing each set of four subsequent points in the contours with their coordinate averaged point.

2.3 Constrained Delaunay tesselation and Chordal Axis Transform

The constrained Delaunay tessellation of a simple planar polygon (contour) is a decomposition of a polygon into triangles, such that the circum-circle of each triangle contains no vertex of the polygon inside it that is simultaneously visible to two vertices of the triangle[3]. Note, that the CDT of the contours is the key step that allows for the shape feature extraction.

In Fig. 5, we transform through the CDT the spectral pixel information of our given micrograph into an affine geometric description. Our previous[4,5] and ongoing[11] work on 2-D shape analysis has amply demonstrated the value of Delaunay triangulations in obtaining structurally meaningful decomposition of shapes into simpler components, much along the lines the human visual system parses complex shapes. 2-D shapes can be decomposed into limbs and torsos[4,5], which are generic shape components. This decomposition is accomplished by applying the CAT.

The triangles originating from the Delaunay triangulation can be classified into three types, namely those with two external (i.e., polygonal boundary) edges, those with one external edge, and those with no external edges. Each kind of triangle carries morphological information about the local structure of the shape's enclosing polygon. Accordingly, they are given different names. A triangle with two external edges marks the termination of a "limb" or a protrusion of the polygon and is called a *termination triangle* or a *T-triangle*. A triangle with one external edge constitutes the "sleeve" of a "limb" or protrusion, signifying the prolongation of the polygon, and is called a *sleeve triangle* or *S-triangle*. Finally, a triangle that has no external edge determines a junction or a branching of the polygon, and is accordingly called a *junction triangle* or a *J-triangle*.

In Fig. 6 and in Fig. 9, we show the *T*-, *J*-, and *S*-triangles for the walls/struts and the large void of the polymeric foam, respectively, with different shades of grey. The brightest triangles are *S*-triangles, whereas the darkest triangles are *T*-triangles. The remaining triangles shown are *J*-triangles. A "limb" is a chain complex of pairwise adjacent triangles, which begins with a junction triangle and ends with a termination triangle. A "torso" is a chain complex of pairwise adjacent triangles, which begins and ends with a junction triangle[4,5].

In Fig. 7 and in Fig. 10, we show the CAT skeletons for the walls/struts and the large void of the polymeric foam, respectively; whereas in Fig. 8 and in Fig. 11, we show their morphologically pruned versions, i.e., structurally insignificant shape features have been removed while preserving the local metrical features of the shapes under consideration (for more detail on the pruning process, please, cf., Refs. 4 and 5). Each arc of the skeletons represents a simplical chain complex of either a limb or a torso, respectively.

The statistical shape properties of the foams struts and walls are at this stage ready for their computation (cf., Section 2.5

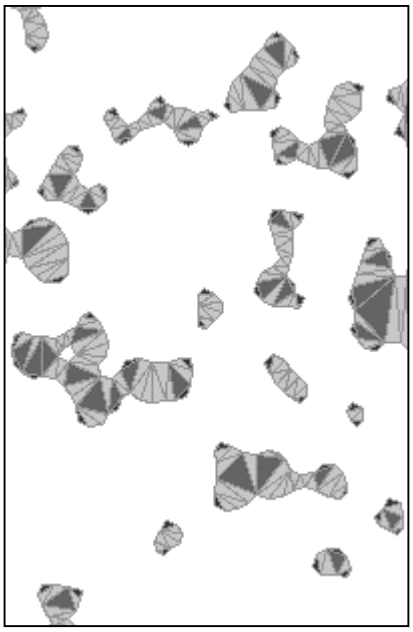

Figure 6: J-, S-, and T-triangles (walls)

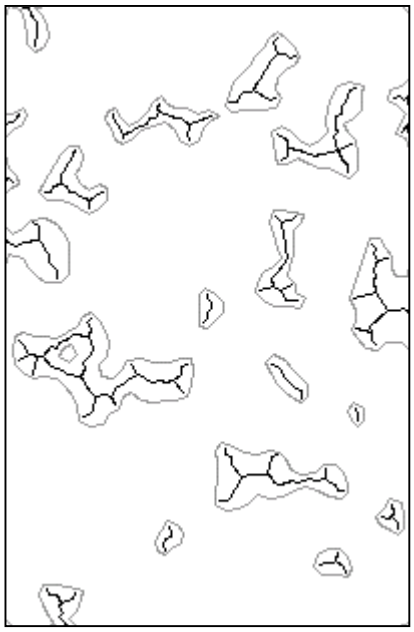

Figure 7: CAT skeleton (walls)

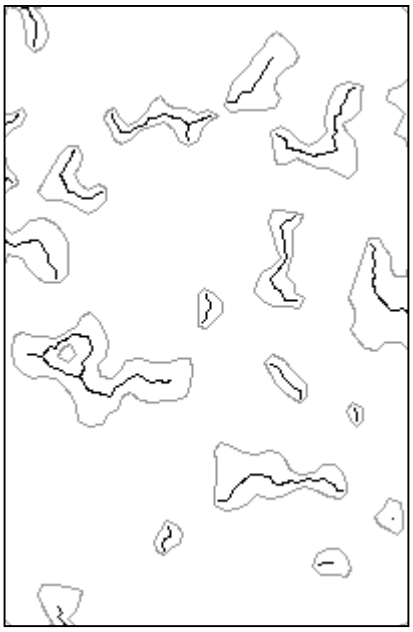

Figure 8: pruned CAT skeleton (walls)

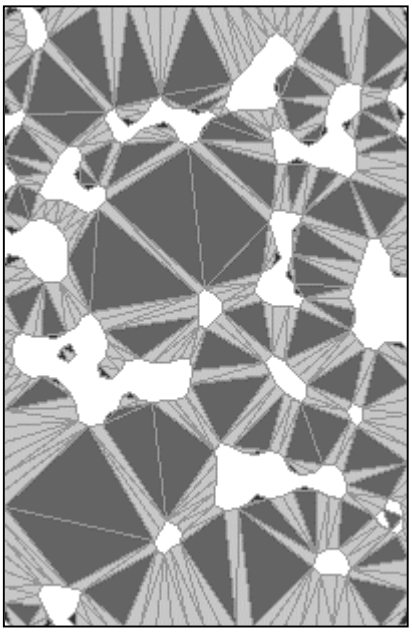

Figure 9: J-, S-, and T-triangles (void)

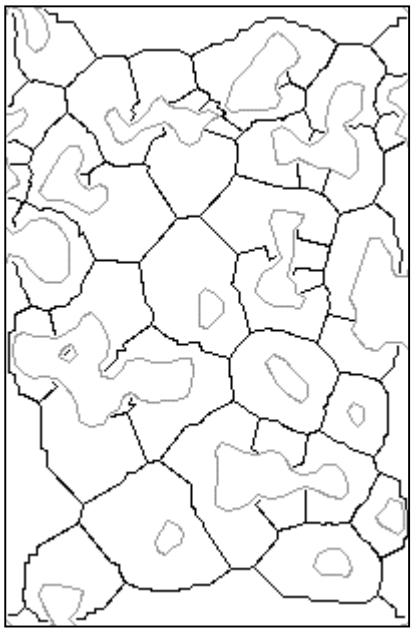

Figure 10: CAT skeleton (void)

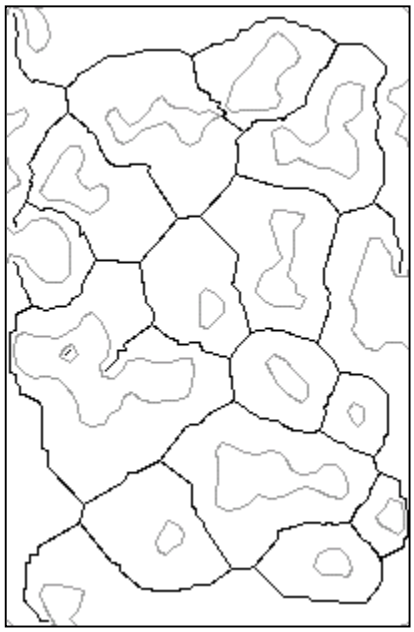

Figure 11: pruned CAT skeleton (void)

"Material statistics"). On the contrary, the foams large void requires further image processing.

2.4 Decomposition of the large void

The polymeric foams large void consists of a complicated network (cf., Fig. 11) of merged, mostly convex shaped single void cells. For the description of, e.g., cell-level stresses, those models addressing the micro-mechanics of the materials under consideration require structural input at the single-cell level. We can provide such information by generating single void cells.

In order to decompose the foams large void into single void cells we make use of the CAT generated limbs and torsos.

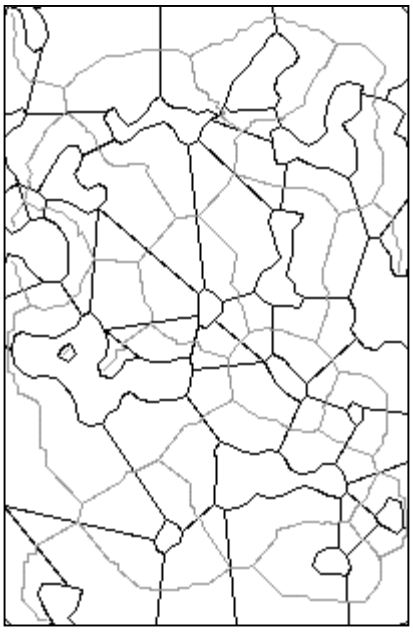

Figure 12: Refined contours (cells)

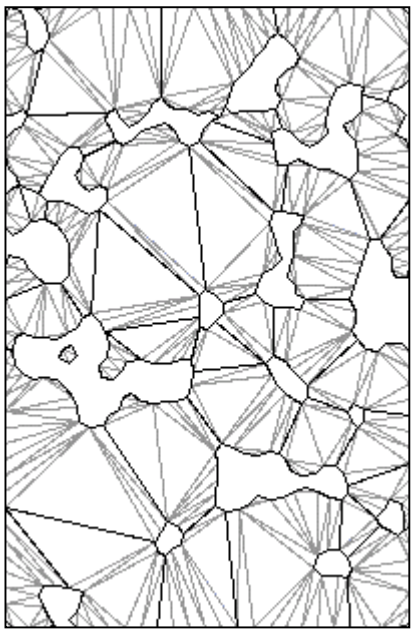

Figure 13: Delaunay grid (cells)

Figure 14: CAT skeleton (cells)

Considering all the CDT edges which connect pairwise adjacent triangles within each torso and limb, we compute a new contour set element by choosing for each torso only the shortest CDT edge, and for each limb the CDT edge which belongs to its only junction triangle, respectively. The result is the original contour edge set and a new edge set, which decomposes the foams large void into single cells. In Fig. 12, we show the original contours and the newly formed refinement edge set, which are superimposed with the large voids pruned CAT skeleton.

In a subsequent step, we reconnect each of the present edge elements to new closed contours, where each of these new contours encloses at this time a single void cell in counter-clockwise orientation. Finally, we again perform a constrained Delaunay tessellation of the original contour point set and the refined contours (cf., Fig. 13) and we also perform a Chordal Axis Transform (cf., Fig. 14), respectively. The repeated application of the CAT enables us to compute the accumulated areas of the individual triangle areas in each void cell through the knowledge of their connectivity within a given void cell. At this time we are prepared for the computation of the statistical shape properties of the foams single void cells.

2.5 Material statistics

In this section, we show statistical distributions for the foams struts/walls and single void cells. In particular, we show in Fig. 15 and in Fig. 16 histograms of areas, aspect ratios, widths and lengths of the corresponding objects. We note, that the micrograph shown in Fig. 1 leads after the applied PCNN image segmentation (cf., Fig. 2) to 1217 strut/wall segments and to 1370 single void cells. We use here a geometric pruning threshold of 60% (cf., Ref.s 4 and 5). The original image consists of 1024x624 pixels.

For the walls/struts we collect the metrical features (areas, lengths, widths) of each limb and torso (after pruning), whereas for the void cells we accumulate in each single void cell the area only. For the walls and struts, their lengths and widths induce their corresponding aspect ratios. On the contrary, for the single void cells we compute a minimum enclosing rectangle around each cell, so that the known area of the cells and the aspect ratio of the minimum enclosing rectangle around each cell induce the cells widths and lengths, respectively. The aspect ratios are normalized such that they always fall into the range between 0 and 1.

3. SUMMARY

In summary, our algorithms transform the spectral pixel information of a micrograph into an affine geometric description, which allows us to analyze the morphology of cellular solids. Our algorithms are superior to many common[12] pixel based shape thinning (skeletonization) methods, because our geometric approach produces high-level shape constituents, i.e., limbs and torsos, which are the basis for the here presented morphological shape manipulation of the polymeric foams large void.

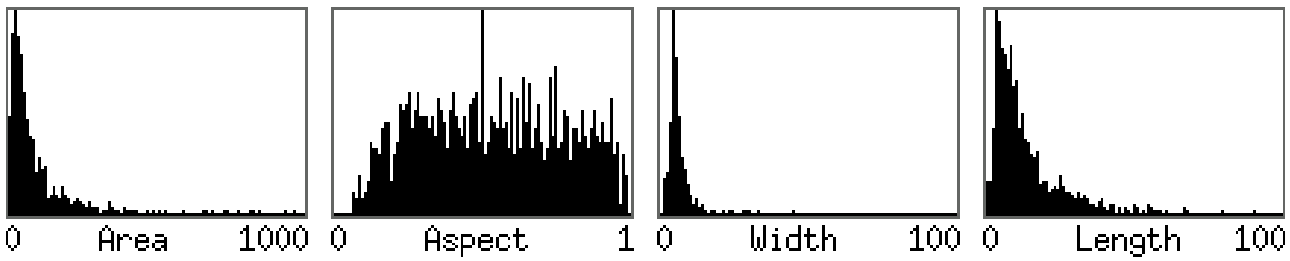

Figure 15: Histograms of areas, aspect ratios, widths and lengths for wall material (1 unit = 1 pixel)

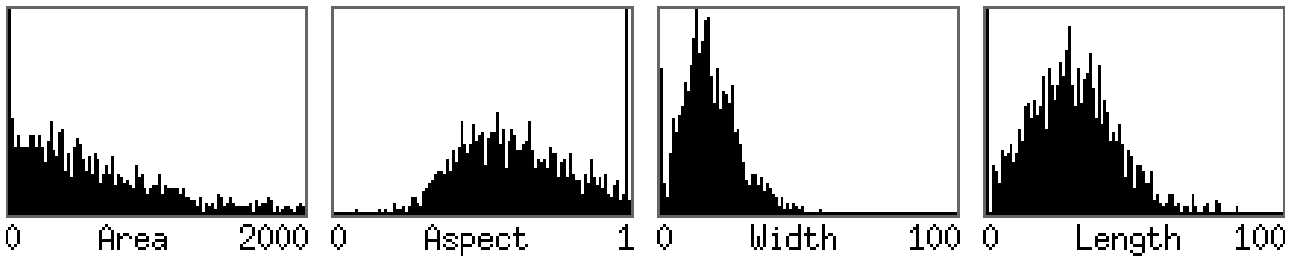

Figure 16: Histograms of areas, aspect ratios, widths and lengths for foam voids (1 unit = 1 pixel)

ACKNOWLEDGEMENTS

This work has been supported by the Department of Energy.

REFERENCES

1. M. W. Schraad, F. H. Harlow, "The Mechanical Response of Polymeric Foams", *T Special Feature 2001*, Supplement to the T-Division Self-Assessment for 2000, May 2001, LA-UR-01-1847, p. 9.
2. A. N. Skourikhine, L. Prasad, B. R. Schlei, "A neural network for image segmentation", *Proceedings of SPIE 2000*, Vol. **4120**, pp. 28 - 35.
3. P. L. George and H. Borouchaki, *Delaunay Triangulation and Meshing*, Hermes, 1998.
4. L. Prasad, "Morphological Analysis of Shapes", *CNLS Newsletter*, No. **139**, July `97, LALP-97-010-139, Center for Nonlinear Studies, Los Alamos National Laboratory.
5. L. Prasad, R. Rao, "A Geometric Transform for Shape Feature Extraction", *Proceedings of SPIE 2000*, Vol. **4117**, pp. 222 – 233.
6. R. Eckhorn, H. J. Reitböck, M. Arndt, P. Dicke, "Feature linking via synchronization among distributed assemblies: simulations of results from cat visual cortex", *Neural Computation*, **2**, pp. 293 – 307, 1990.
7. M. Stöcker, H. J. Reitböck, R. Eckhorn, "A neural network for scene segmentation by temporal coding", *Neurocomputing*, **11**, pp. 123 – 134, 1996.
8. courtesy: M. W. Schraad and F. H. Harlow, Los Alamos National Laboratory, Theoretical Division, T-3, P.O. Box 1663, MS B216, Los Alamos, NM 87545, U.S.A.
9. B. R. Schlei, "DICONEX - Dilated Contour Extraction Code, Version 1.0", Los Alamos Computer Code LA-CC-00-30, Los Alamos National Laboratory, 2000; for more detail check the website http://www.nis.lanl.gov/bschlei/eprint.html.
10. B. R. Schlei, L. Prasad, "A Parallel Algorithm for Dilated Contour Extraction from Bilevel Images", Los Alamos Preprint LA-UR-00-309, Los Alamos National Laboratory, cs.CV/0001024, 2000.
11. B. R. Schlei, L. Prasad, A. N. Skourikhine, "Geometric morphology of granular materials", *Proceedings of SPIE 2000*, Vol. **4117**, pp. 196 - 201.
12. J. R. Parker, *Algorithms for Image Processing and Computer Vision*, John Wiley & Sons, 1997.